In press in Geolgy, July 1999

Birth of a fault: Connecting the Kern County and Walker Pass, California, earthquakes

Gerald W. Bawden

Andrew J. Michael

U.S. Geological Survey, M.S. 977, Menlo Park, California 94025, USA

Louise H. Kellogg

Geology Department, University of California, Davis, California 95616, USA

ABSTRACT

A band of seismicity transects the southern Sierra Nevada range between the northeastern end of the 1952 M_w (moment magnitude) 7.3 Kern County earthquake and the site of the 1946 M_w 6.1 Walker Pass earthquake. Relocated earthquakes in this band, which lacks a surface expression, better delineate the northeast-trending seismic lineament and resolve complex structure near the Walker Pass mainshock. Left-lateral earthquake focal planes are rotated counterclockwise from the strike of the seismic lineament, consistent with slip on shear fractures such as those observed in the early stages of fault development in laboratory experiments. We interpret this seismic lineament as a previously unrecognized, incipient, currently blind, strike-slip fault, a unique example of a newly forming structure.

INTRODUCTION

The initial stages of fault development have been recognized in laboratory experiments, but not at seismogenic depths. To fully understand how faults initially develop and begin to evolve, one needs to first recognize and then observe the emerging structure. Recognizing the birth of a fault requires a priori knowledge of the regional tectonics, geologic structure, and seismic history. This information is needed to assess the likelihood that earthquake hypocenters that occur far from

known faults represent new fault formation rather than slip at depth on existing structures. Furthermore, young faults may begin as blind structures, which makes them difficult to recognize.

The 1983 M_W (moment magnitude) 6.4 Coalinga, 1987 M_W 6.0 Whittier Narrows, and 1994 M_W 6.7 Northridge earthquakes revealed the significance of blind thrust faults in California. Unlike the San Andreas fault, blind faults are difficult to recognize because they lack visible, surface features. Even after a blind fault is identified, it is difficult to determine whether the fault is active (Lettis et al., 1997). However, no active blind strike-slip faults have been documented anywhere, with possible exceptions at the Long Valley caldera and the Mount Lewis seismic trend in California (Cockerham and Pitt, 1984; Zhou et al., 1993). We present evidence for an incipient, blind, strike-slip fault in California's southern Sierra Nevada that is associated with the 1946 Walker Pass earthquake.

OBSERVATIONS

We studied the diffuse band of seismicity that is located between two large, historic, earthquakes: the 1946 M_W 6.1 Walker Pass earthquake on the northern end of the lineament and the 1952 M_W 7.3 Kern County earthquake that ruptured along the White Wolf fault on the southern end of the lineament (hereafter we refer to the seismic lineament as the Scodie lineament – Fig. 1). The idea that these earthquakes were possibly tectonically connected was loosely suggested by (Richter, 1958), and the existence of the lineament was later observed by (Qian et al., 1989). Previous seismicity studies (Chakrabarty and Richter, 1949; Gardner, 1964) and geologic maps (Dibblee and Chesterman, 1953; Saleeby and Busby-Spera, 1986; Ross, 1989) of the area do not show a surface expression of a fault, geologic structure, or tectonic landform corresponding to the Scodie lineament. The regional geology is a mix of Mesozoic granitic rocks with isolated, north-trending pre-Cretaceous metamorphic terranes. The trend of the lineament is at about a 40° angle to the prominent north-trending fabric of the Sierra Nevada (Ross, 1986); therefore the local geology provides several unambiguous piercing points along the lineament at which displacement could be resolved.

We relocated and calculated focal mechanisms for the earthquakes between the northern end of the White Wolf fault and the 1946 main shock. Both the seismic networks in the vicinity of the Scodie lineament, and the techniques used to relocate earthquakes have significantly improved since the last detailed seismic studies were conducted for the area. The Scodie lineament falls on the border between the Northern California and Southern California Seismic Networks, and both networks operate seismographic stations in the Sierra Nevada. We took advantage of the rich data sets from these overlapping seismic networks by merging short-period P-wave phase data from both networks for 7274 earthquakes that occurred between September 1976 and March 1998. To better resolve the characteristics of the seismic lineament, we used the method of joint hypocentral determination to obtain new seismic station traveltime corrections (Kissling, 1988) and then relocated the earthquakes (Klein, 1989) using the velocity model derived by Jones and Dollar (1986). To minimize erroneous earthquake locations, we excluded earthquakes that were recorded at fewer than 15 seismic stations, had an RMS uncertainty of >0.1 s, had a relative horizontal position uncertainty of >0.35 km, and a relative vertical position uncertainty of >0.9 km. Similarly, focal mechanisms were calculated for all of the magnitude 2.0 and greater earthquakes that had a minimum of 12 phase readings (Reasenberg and Oppenheimer, 1985). To minimize potential problems with low amplitude or improper ray traced refracted waves, we gave lower weight to poor quality arrivals. All focal mechanisms were visually and statistically inspected, and unresolveable focal mechanisms were removed from the data set.

The improved hypocenters define a narrower Scodie seismic lineament (Fig. 1A), with earthquakes clustered at the ends and in the center of the lineament. Most earthquakes along the Scodie lineament have strike-slip fault-plane solutions, and their focal depths are greater than 4 km (Fig. 1, B and C). If these earthquakes are aligned with the overall trend of the seismic lineament, then the preferred direction of slip would be left-lateral strike slip along the northeast-striking fault planes (Fig. 2A).

Seismicity in the Scodie seismic lineament can be characterized as three sections (Fig. 1, A-C). The southwest section contains a mixture of left-lateral strike-slip events and reverse events that are

located in the aftershock zone of the 1952 Kern County earthquake. Most (84 %) of these shocks are strike slip events, presumably left-lateral slip associated with the White Wolf fault. The central region of the lineament forms a zone of diffuse events with clusters of earthquakes near the axis of the lineament. Nearly all earthquakes in this section are consistent with left-lateral strike slip subparallel to the lineament. Earthquakes along the northern section of the Scodie lineament are predominately strike-slip events with scattered normal-slip events (Fig. 2). The majority of the earthquakes in this region are in the vicinity of the 1946 Walker Pass earthquake and suggest a complex series of en echelon fault segments. Two such fault segments coalesce at depth as well as along strike (Fig. 2).

The microseismicity in the Walker Pass earthquake region suggests that the main shock may have occurred on a northeast–trending southeast-dipping fault, thereby helping to constrain the variety of focal mechanisms that have been calculated for the event. Focal mechanisms for the 1946 Walker Pass earthquake have been calculated by a variety of techniques, all trying to exploit the few available seismic readings (Chakrabarty and Richter, 1949; Dollar and Helmberger, 1985; Gardner, 1964; Burdick, 1996). Conclusions from these studies suggest that the main shock occurred on either a north-trending normal fault or a northeast-trending left-lateral strike-slip fault (Fig. 2). On the basis of trends in the microseismicity near the main shock, we favor the strike-slip focal mechanism and suggest that the northeast-trending nodal plane is the fault plane.

INTERPRETATIONS

On the basis of the seismicity pattern and focal mechanisms, we infer that the Scodie lineament is likely a left-lateral shear zone. Although the central section contains only diffuse seismicity, this could be consistent with an incipient fault, and the clear activity at both ends should evolve, with time, toward a connected throughgoing fault. The lack of a surface expression associated with the seismic lineament may be because it is a young fault that has had little throw.

To determine whether the Scodie lineament is an incipient feature, we searched for evidence of Riedel shear; faults and fractures that form at an oblique angle (about 10°-35°) to the maximum

direction of shear in material without a continuous fault surface. In laboratory experiments, Riedel shear fractures form during the early stages of a fault's development, with the angle between the maximum shear plane and the Riedel shear fractures a function of the angle of internal friction (Bartlett et al., 1981; Schreurs, 1994). For well-developed faults, we would expect that the T-axis orientations for earthquakes near the fault to be oriented 45° from the direction of maximum shear. However, if Riedel shear is present, then we would anticipate as much as a 35° counterclockwise rotation of the T-axis orientations from this expected azimuth (Fig. 1D). For the Scodie lineament, we calculated T-axis azimuths from strike slip focal mechanisms that lie within 10 km of the Scodie lineament and found that the majority of the T-axes are not parallel to the lineament– instead they are rotated counterclockwise (Figs. 3, 1B, and 1D).

To evaluate the significance of the observed T-axis rotation within the Scodie lineament, we conducted a statistical test of skewness of the T-axis data about the expected T-axis azimuth. We assume that errors in the focal mechanisms are distributed symmetrically about the true T-axis, an assumption that could be invalid if the distribution is not symmetric because of poor station distribution, improperly traced rays, or noisy data. We binned the data into two groups that contained T-axis trends less than and greater than the expected T-axis azimuth. We also truncated the distributions at ±35° from the expected direction. Without Riedel shear, the errors should be symmetric about the expected direction (45° from the strike of the fault), so the number of events in the two bins should be described by the binomial distribution. In contrast, if Reidel shear was present, it would show up as skewness in the distribution; i.e., the number of events in either bin is larger than would be found under the null hypothesis of no Reidel shear.

We found that the observed T-axis orientations are inconsistent with pure left-lateral slip along the Scodie lineament, but they are consistent with Riedel shear along the lineament (Fig. 3A, Table 1). The two trends at the northern end of the Scodie lineament (Fig. 2) broaden the distribution of T-axis azimuths, but are not responsible for the rotation of the T-axes from the expected trend. In contrast, at the Parkfield section of the San Andreas fault, observed T-axis orientations for strike-slip earthquakes calculated with both a one-dimensional (1-D) (Northern California Earthquake

Data Center) and a three-dimensional (3-D) seismic velocity model (Eberhart-Phillips and Michael, 1993) are not skewed (Fig. 3B and Table 1), indicating that Reidel shear is not present on this older, well-developed fault. Because the 1-D and 3-D seismic velocity models produced nearly identical results even though the Parkfield region has significant 3-D structure (Eberhart-Phillips and Michael, 1993), we do not expect that uncertainties in ray tracing affected the Scodie lineament results. Thus, at the 99.9% confidence level, there is evidence for Reidel shear along the Scodie lineament. This finding suggests that the Scodie lineament has the characteristics of a young, anastomosing fault and not a continuous structure.

TECTONIC IMPLICATIONS AND CONCLUSIONS

The close proximity and orientations of the Scodie seismic lineament and the White Wolf fault suggest that these two structures are related. The seismic lineament may represent an extension or propagation of the White Wolf fault towards the northeast. The big bend segment of the San Andreas fault is a restraining bend that is not oriented parallel to the Pacific–North American plate motion. The White Wolf and Garlock faults both accommodate the big bend transpression; oblique reverse slip on occurs the White Wolf fault, and left-lateral slip occurs on the Garlock fault (Fig. 1A-inset). It is possible that the Garlock fault has shifted south, with the North American plate, beyond the portion of the big bend whose orientation deviates the most from the Pacific–North American plate motion. If so, then this kink in the San Andreas fault might have caused the White Wolf fault to lengthen to accommodate further slip, extending the White Wolf fault to form the Scodie seismic lineament. No older analogues to the Scodie seismic lineament and Garlock fault are known, perhaps because the big bend is not old enough (Atwater and Stock, 1998) to have produced a prior fault with a similar orientation.

As discussed above, the Scodie lineament may represent an incipient fault that is a product of the tectonic evolution in the big bend region. We propose that the diffuse band of strike slip earthquakes that connects the White Wolf fault to the Walker Pass seismicity is an embryonic fault. The 15° rotation of the focal mechanisms from the trend of the lineament is consistent with

laboratory observations of fault development. Thus we have extended the Riedel shear model from laboratory-scale experiments to in situ observations at seismogenic depths.

ACKNOWLEDGMENTS

Support provided by National Science Foundation grant EAR-97-06690 and a Presidential Faculty Fellowship to L. Kellogg. We thank R. Stein, C. Jones, A. Nur, L. Jones, E. Moores, J. Savage, and W. Thatcher for reviews of the manuscript. We also thank R. Bürgmann, A. Donnellan, K. Hafner, L. Jones, D. Oppenheimer, J. Sauber, and R. Twiss for comments, discussions, and technical assistance. The seismic data were obtained through the Northern California Earthquake Data Center, a joint project of the Northern California Seismic Network, U.S. Geological Survey, Menlo Park, and the Seismological Laboratory, University of California, Berkeley, and through the Southern California Seismic Network, a joint project of the U.S. Geological Survey, Pasadena and the Seismological Laboratory, Pasadena.

REFERENCES CITED

Atwater, T., and Stock, J., 1998, Pacific-North America plate tectonics of the Neogene southwestern United States; an update: International Geology Review, v. 40, p. 375-402.

Bartlett, W.L., Friedman, M., and Logan, J.M., 1981, Experimental folding and faulting of rocks under confining pressure: Part IX. Wrench faults in limestone layers: Tectonophysics, v. 79, p. 255-277.

Burdick, L.J., 1996, Historical earthquake sequences: Pasadena, California Institute of Technology, Seismological Laboratory Report, p. 15.

Buwalda, J.P., and St. Amand, P., 1955, Geological effects of the Arvin-Tehachapi earthquake, *in* Oakeshott, G., ed., Earthquakes in Kern County, California during, 1952: California Division of Mines Bulletin 171, p. 41-56.

Chakrabarty, S.K., and Richter, C.F., 1949, The Walker Pass earthquakes and structure of the southern Sierra Nevada: Seismological Society of America Bulletin, v. 39, p. 93-107.

Cockerham, R.S., and Pitt, A.M., 1984, Seismic activity in Long Valley caldera area, California; June 1982 through July 1984, *in* Hill, D., Bailey, R.A., and Ryall, A.S., eds., Proceedings of Workshop XIX; Active tectonic and magmatic processes beneath Long Valley caldera, eastern California, U.S. Geological Survey Open-File Report no. 84-939, p. 493-526.

Dibblee, T.W., Jr., and Chesterman, C.W., 1953, Geology of the Breckenridge Mountain Quadrangle, California: California Division of Mines and Geology, v. 168, p. 1-56.

Dollar, R.S., and Helmberger, D.V., 1985, Body wave modeling using a master event for the sparsely recorded 1946 Walker Pass, California earthquake: Eos (Transactions American Geophysical Union), v. 66, p. 964.

Eberhart-Phillips, D., and Michael, A.J., 1993, Three-dimensional velocity structure, seismicity, and fault structure in the Parkfield region, central California: Journal of Geophysical Research, v. 98, p. 15737-15758.

Gardner, J.K., 1964, Earthquakes in the Walker Pass region, California, and their relation to the tectonics of the southern Sierra Nevada [Doctoral thesis], Pasadena,California Institute of Technology.

Jones, L.M., and Dollar, R.S., 1986, Evidence of basin-and-range extensional tectonics in the Sierra Nevada: the Durrwood Meadows swarm, Tulare County, California (1983-1984): Seismological Society of America Bulletin, v. 76, p. 439-461.

Kissling, E., 1988, Geotomography with local earthquake data: Reviews of Geophysics, v. 26, p. 659-698.

Klein, F.W., 1989, User's guide to HYPOINVERSE, a program for VAX computers to solve for earthquake locations and magnitudes, U.S. Geological Survey Open-File Report no. 89-314, p. 58.

Lettis, W.R., Wells, D.L., and Baldwin, J.N., 1997, Empirical observations regarding reverse earthquakes, blind thrust faults, and Quaternary deformation; are blind thrust faults truly blind?: Seismological Society of America Bulletin, v. 87, p. 1171-1198.

Qian, H., Jones, C.H., and Kanamori, H., 1989, Seismotectonics of the southern Sierra Nevada, California: Early Stages of an Intracontinetal Transform?: Eos (Transactions American Geophysical Union), v. 70, p. 1209.

Reasenberg, P., and Oppenheimer, D.H., 1985, FPFIT, FPPLOT and FPPAGE; Fortran computer programs for calculating and displaying earthquake fault-plane solutions, U.S. Geological Survey Open-File Report no. 85-739, p. 109.

Richter, C.F., 1958, Elementary seismology: San Francisco, W.H. Freeman and Co., Inc, 768 p.

Ross, D.C., 1986, Basement-rock correlations across the White Wolf-Breckenridge-southern Kern Canyon fault zone, southern Sierra Nevada, California, U. S. Geological Survey Bulletin B1651, p. 25.

Ross, D.C., 1989, The metamoprhic and plutonic rocks of the southernmost Sierra Nevada, California, and their tectonic framwork, U. S. Geological Professional Paper 1381, p. 159.

Saleeby, J.B., and Busby-Spera, C., 1986, Fieldtrip guide to the metamorphic framework rocks of the Lake Isabella area, southern Sierra Nevada, California, *in* Dunne, G.C., ed., Mesozoic and Cenozoic structural evolution of selected areas, east-central California, p. 81-94.

Schreurs, G., 1994, Experiments on strike-slip faulting and block rotation: Geology, v. 22, p. 567-570.

Zhou, Y., McNally, C., and Lay, T., 1993, Analysis of the 1986 Mt. Lewis, California, earthquake: preshock sequence- mainshock- aftershock sequence: Physics of the Earth and Planetary Interiors, v. 75, p. 267-288.

Figure 1. A: Relocated earthquakes in southern Sierra Nevada from 1976 to 1998. Aftershocks from Walker Pass earthquake can be still seen in seismicity as band of earthquakes near Scodie Mountains. Seismicity northeast of dashed line is in Coso geothermal field and was not included in this study. Inset location map shows location of major faults in region of the Big Bend of the San Andreas fault. Triangles–seismographic stations. Open box A-A' is location of cross section below. B: Color-coded P and T axes in seismic lineament. Majority of earthquakes in seismic lineament are strike slip (red). North-trending band of seismicity near Lake Isabella has primarily east-west extension (blue), possibly caused by migration of basin-and-range-style extension into southern Sierra Nevada (Jones and Dollar, 1986). Gold oblate curve surrounding northern end of White Wolf fault is approximate aftershock zone for 1952 Kern County earthquake. Box near A' is location map for Figure 2. C: A-A' cross section along Scodie lineament. Symbols and colors represent the type of earthquake [see key in B]. Black points are earthquakes that have good locations, but whose focal mechanism is uncertain. Orange bars represent possible rupture extent for 1946 Walker Pass earthquake (from aftershock locations) and observed surface rupture from the 1952 Kern County earthquake (Buwalda and St. Amand, 1955). D: Schematic diagram of T-axis and focal-mechanism orientations for a well-developed fault and a fault that has Riedel shear. Both faults are shown with same orientation as Scodie lineament.

Figure 2. Focal mechanisms and earthquake foci surrounding Walker Pass earthquake. This region contains complex zone of left-stepping, left-lateral strike-slip faults and fault splays with broadly distributed extensional earthquakes (blue). In cross-section B-B', main fault trace is well-defined steeply dipping fault that begins at about 4 km depth and then shallows with increasing depth. Southeastern fault splay on cross section is represented as wide (2 km) zone of seismicity that joins with main fault. Since cross section is perpendicular to main fault, not to fault splay, distribution about fault splay is artificially widened. The two focal mechanisms are representative of existing solutions for Walker Pass earthquake (Burdick, 1996). Open circles–aftershocks from 1946 earthquake (Chakrabarty and Richter, 1949), yellow star–main shock. Location shown by box in Figure 1B near Scodie Mountains. Light blue lines are suggested fault-plane locations. Open box labeled B-B' is location for cross section (inset).

Figure 3. Strike-slip T-axis orientation histograms for (A) Scodie seismic lineament and (B) and Parkfield 1-D data. Bold vertical line is expected T-axis orientation, which is at 45° from strike of fault.

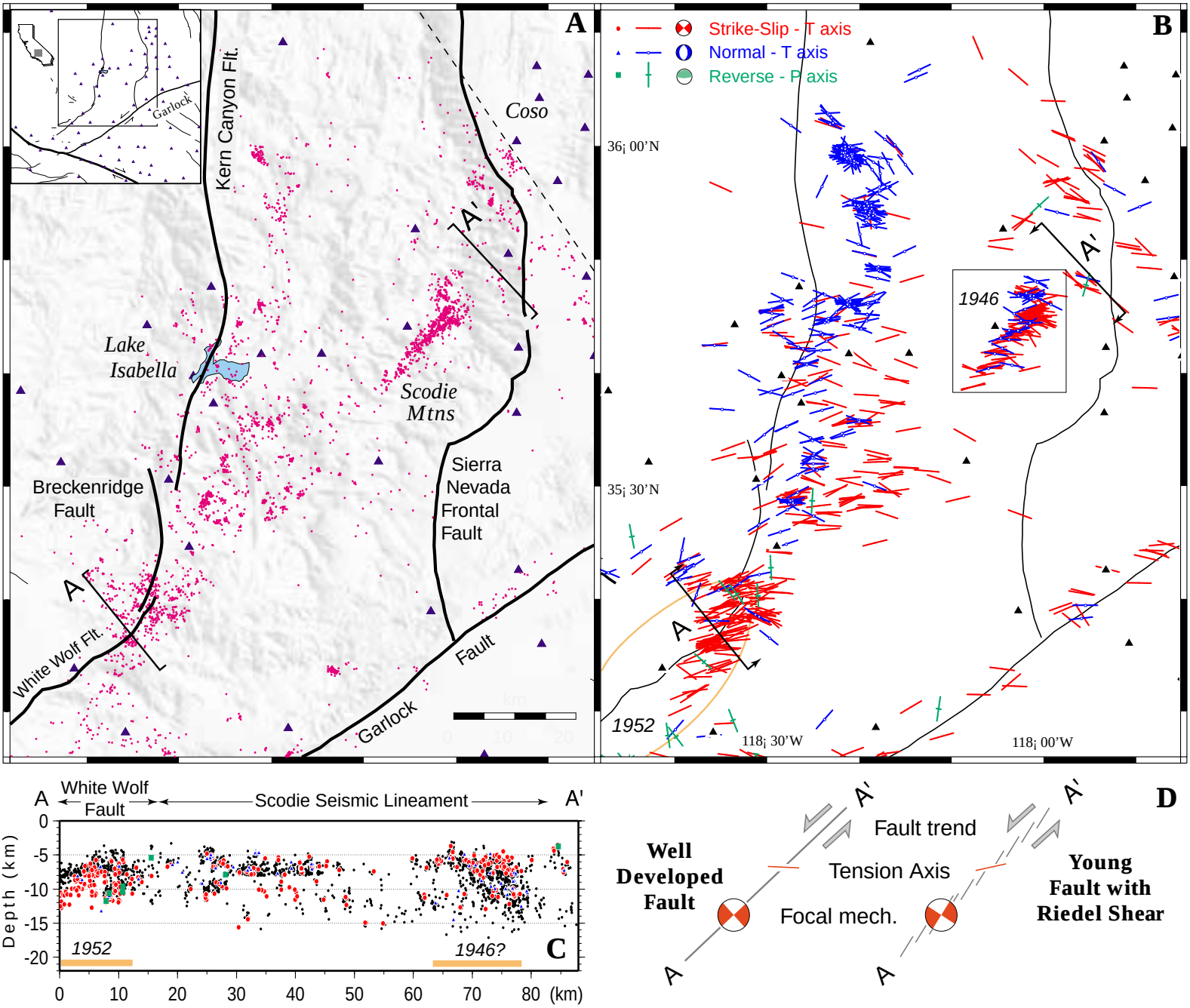

Bawden *et al.*, Figure 1

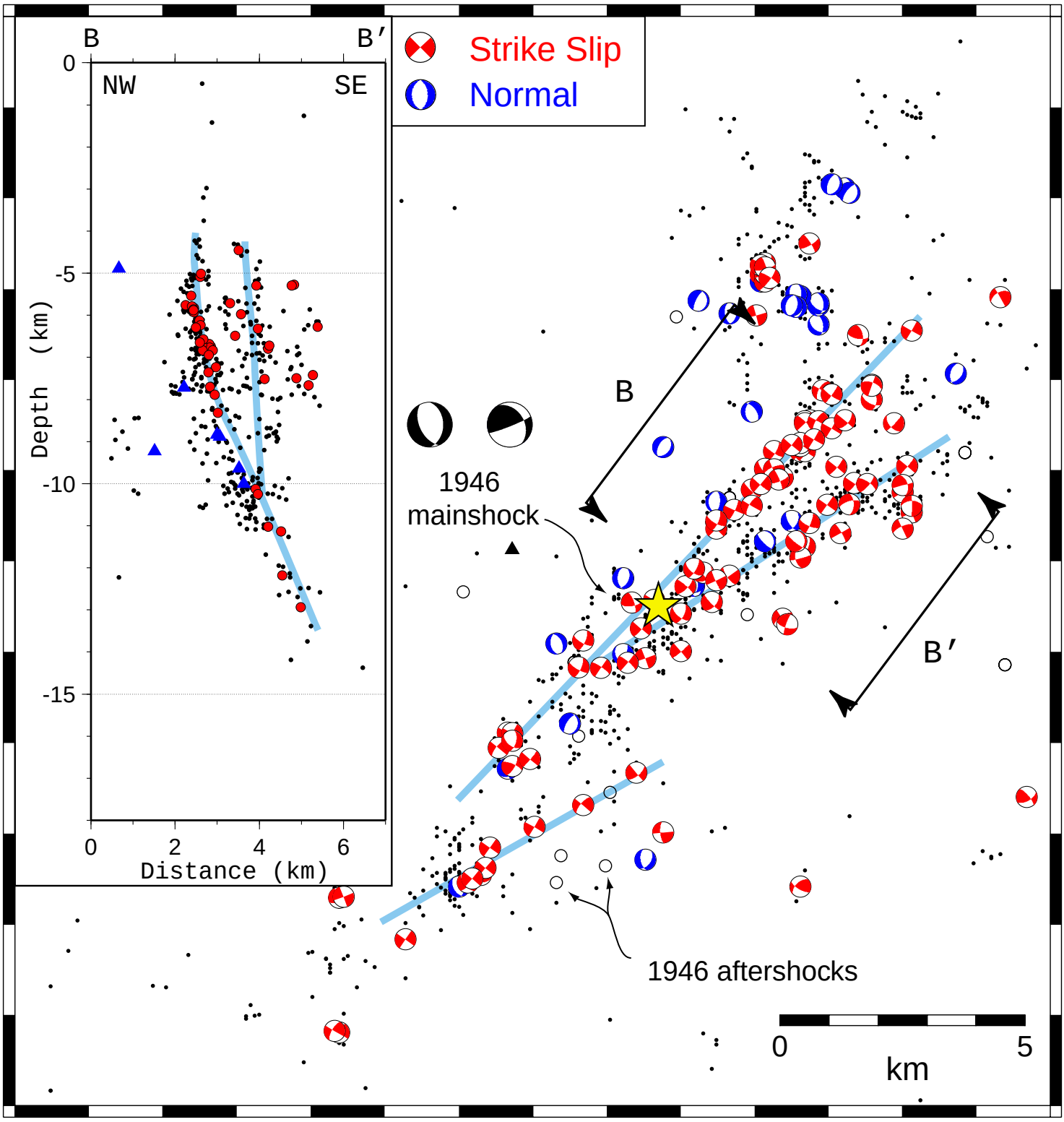

Figure 2, Bawden *et al.*

MS# G15244A

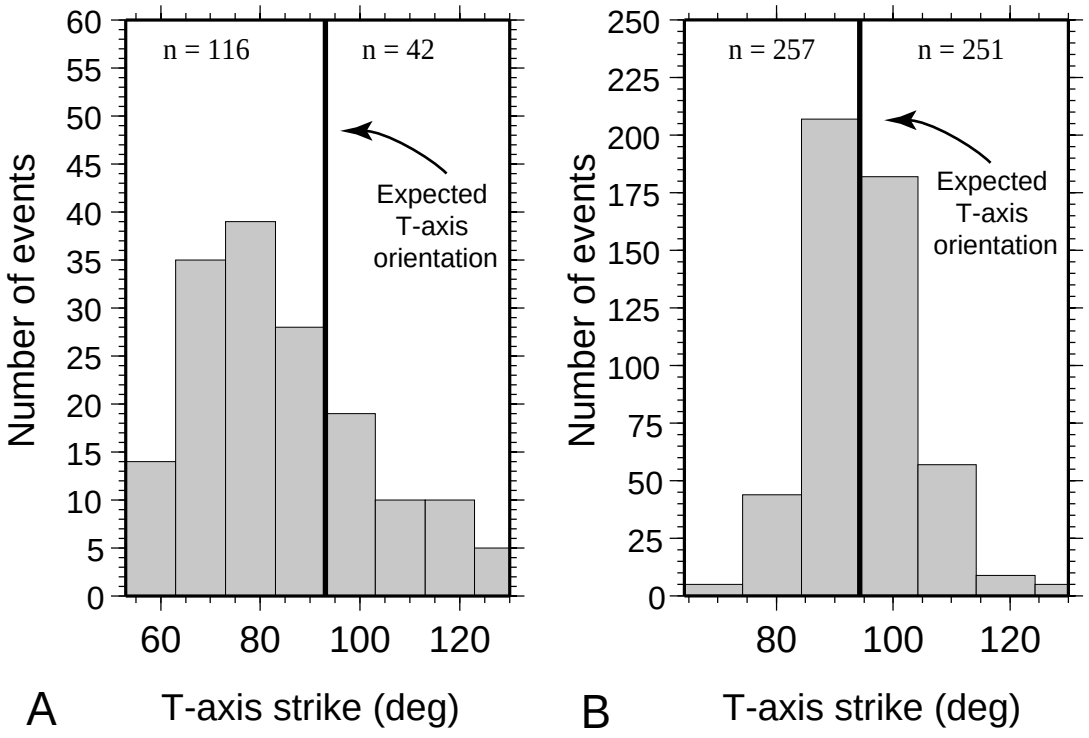

Figure 3, Bawden *et al.*
MS# G15244A